

Group Editing : Edit Multiple Images in One Go

Yue Ma¹, Xinyu Wang², Qianli Ma^{3§}, Qinghe Wang[✉], Mingzhe Zheng¹, Xiangpeng Yang⁴,
 Hao Li², Chongbo Zhao², Jixuan Ying², Harry Yang¹, Hongyu Liu^{1✉}, Qifeng Chen¹
¹ HKUST ² THU ³ SJTU ⁴ University of Technology Sydney

Project: <https://group-editing.github.io/>

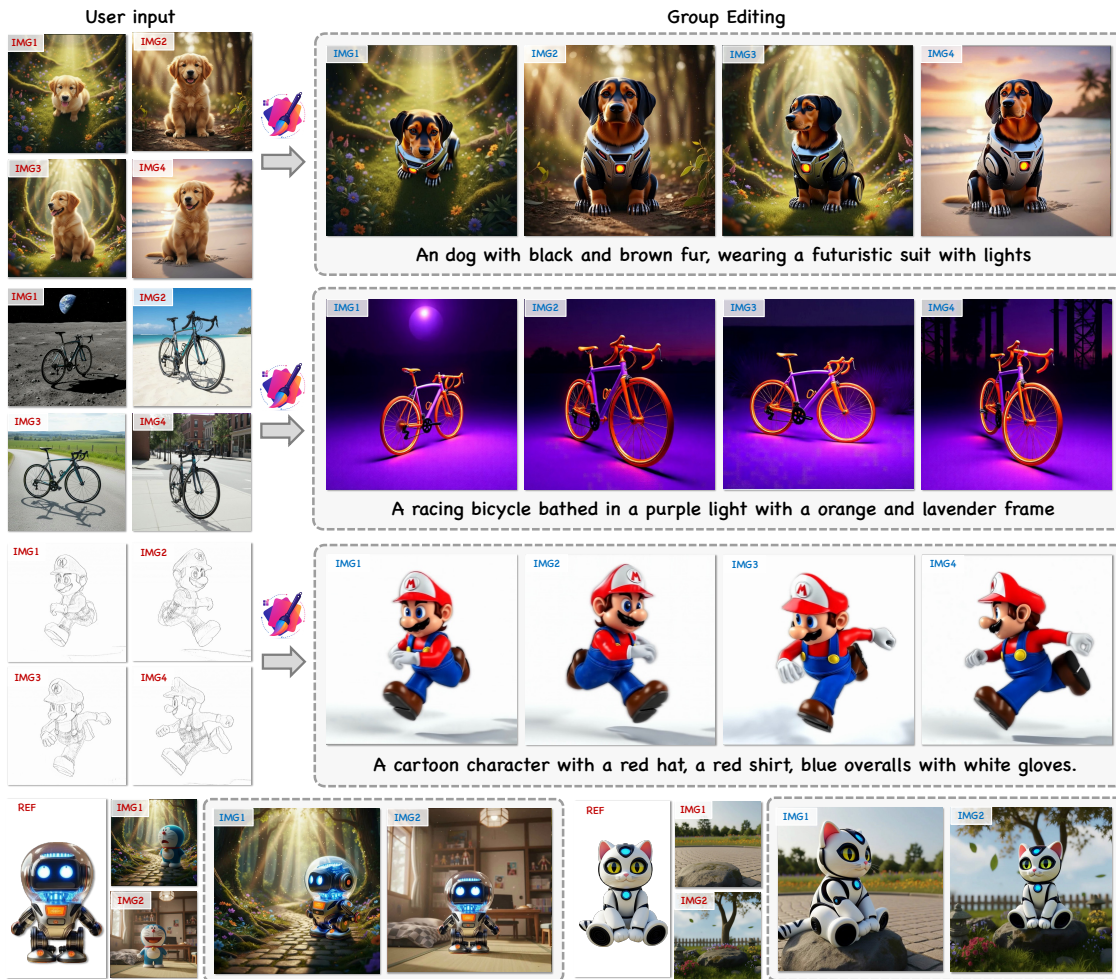


Figure 1. **Gallery of proposed method.** We propose the *GroupEditing*, which aims to apply consistent and unified modifications across a set of related images. Our *GroupEditing* supports local and global editing, colorization, customization, and insertion among image groups.

✉ Corresponding author.
 § Project leader

Abstract

In this paper, we tackle the problem of performing consistent and unified modifications across a set of related images. This task is particularly challenging because these images may vary significantly in pose, viewpoint, and spatial layout. Achieving coherent edits requires establishing reliable correspondences across the images, so that modifications can be applied accurately to semantically aligned regions. To address this, we propose GroupEditing, a novel framework that builds both explicit and implicit relationships among images within a group. On the explicit side, we extract geometric correspondences using VGGT, which provides spatial alignment based on visual features. On the implicit side, we reformulate the image group as a pseudo-video and leverage the temporal coherence priors learned by pre-trained video models to capture latent relationships. To effectively fuse these two types of correspondences, we inject the explicit geometric cues from VGGT into the video model through a novel fusion mechanism. To support large-scale training, we construct GroupEditData, a new dataset containing high-quality masks and detailed captions for numerous image groups. Furthermore, to ensure identity preservation during editing, we introduce an alignment-enhanced RoPE module, which improves the model’s ability to maintain consistent appearance across multiple images. Finally, we present GroupEditBench, a dedicated benchmark designed to evaluate the effectiveness of group-level image editing. Extensive experiments demonstrate that GroupEditing significantly outperforms existing methods in terms of visual quality, cross-view consistency, and semantic alignment.

1. Introduction

Group-image editing aims to achieve consistent and unified content creation across a set of related images. Unlike single-image editing [4, 7, 42, 43, 52, 63], which only focuses on generating plausible results for an individual image, this task requires maintaining editing coherence among multiple images in both appearance and structure. It is crucial in many emerging applications. For example, in virtual content creation, maintaining coherent edits across images ensures identity integrity for digital avatars and characters [2, 29]. In digital commerce, consistent product depiction across angles improves consumer trust and supports robust visual recommendations. Moreover, this task also improves both the efficiency and quality of downstream tasks such as photo retouching [11], data augmentation for personalization [47], and 3D reconstruction [22, 56].

While consistent editing is highly desirable, ensuring coherence across diverse images remains a challenge. Previous editing approaches typically operate on a per-image

basis, resulting in variations that undermine the uniformity necessary for practical applications [4, 7, 10, 35, 38, 42, 43, 54, 61, 63, 65, 66]. Optimization-based frameworks [21, 61, 63] attempt to edit one image and propagate the modifications across images, but the lack of robust generalization leads to artifacts and inconsistency. Recent optimization-free methods [3] rely on semantic correspondences from attention features and open-sourced tracking tools, but their application is limited to a small number of images. A major challenge stems from the lack of high-quality training pairs and sufficient constraints to maintain uniformity, especially in geometrically complex scenes (e.g., identifying the ‘left eye’ in various images or tracking a logo on a T-shirt during a 30-degree rotation), which hinders generalization.

In this paper, we revisit the problem of group-image editing and explore the question: *What is an appropriate representation for establishing correspondence in this task?* We approach this question from two key observations. **i) Implicit correspondence:** Compared to image models, video models inherently possess stronger generative priors and temporal coherence. Trained on large-scale sequential data, video models learn to capture not only semantic continuity but also the spatial transformations of objects. This implicit correspondence allows models to maintain both temporal and spatial consistency naturally, making video models a promising foundation for consistent group-image editing. **ii) Explicit correspondence:** We observe that the semantic correspondence in the video model alone is insufficient. While attention-based matching or pre-trained feature correspondences can align semantic regions (e.g., “face to face”, “object to object”), they often fail in geometrically complex scenes where local structures undergo rotation, deformation, or occlusion. To migrate this, we leverage explicit correspondences extracted from the VGGT [56], which offers dense matching quality, exemplifying the advantage of strong feature representations.

Motivated by the observations above, we propose GroupEditing, a novel training-based framework for consistent group-image editing. Instead of treating each image independently, we reformulate a set of related images as *pseudo video frames*, enabling the model to inherit the temporal and geometric priors learned by large-scale video models. The explicit correspondence representation is obtained from the VGGT [56] encoder and injected into the video model [53] with the proposed fine-grained geometry-enhanced RoPE (Ge-RoPE). The identity-enhanced RoPE is designed for consistent identity preservation. Additionally, to enable large-scale training, we develop a scalable dataset pipeline leveraging various advanced vision models [12, 25, 28, 57], constructing the largest group-image editing dataset, *GroupEditData*, and benchmark, *GroupEditBench*, with over 800 groups of images, each featuring

precise segmentation masks and detailed text descriptions. We further demonstrate the potential of *GroupEditing* by establishing an inpainting-based image editing pipeline that delivers promising results. To evaluate the effectiveness of our approach, we compare *GroupEditing* with prior state-of-the-art (SOTA) baselines. *GroupEditing* consistently outperforms all competitors, achieving superior visual quality. In summary, our primary contributions are:

- We tackle the problem of performing consistent multiple image editing, and propose *GroupEditing*, the first training-based framework that reformulates a set of related image sequences as pseudo video frames.
- To enable consistent group-image editing, we introduce geometry-enhanced RoPE that integrates both implicit and explicit correspondence, along with an identity-enhanced RoPE module for robust identity alignment.
- To train our model, we develop a dataset pipeline, construct GroupEditData (> 7K groups) and GroupEditBench, each with precise masks and detailed captions.
- Experiments show that *GroupEditing* achieves SOTA performance across four metrics, including visual quality, editing consistency, and semantic alignment, outperforming baselines on the GroupEditBench.

2. Related Work

Generative models for image editing. Image editing, a long-standing problem with broad practical impact, has been substantially advanced by generative modeling [1, 15, 18, 20, 23, 24, 34, 37, 39, 41, 45]. Recent advances in diffusion models have enabled highly effective editing paradigms [4, 6, 7, 14, 27, 42, 52, 55, 62]. Existing techniques can be broadly divided into inference-time zero-shot methods that edit images by manipulating the diffusion process itself [6, 42, 52] and training-based methods, which achieve editing by fine-tuning latent diffusion models [4, 43, 44, 63]. However, these methods remain tailored to single-image editing and, despite efforts to enforce consistency [6, 42, 58], they are constrained to small inputs and often break down under complex geometric variation, which is partly due to scarce paired training data. To address this, we formalize *Group-Image Editing* and introduce *GroupEditing*, a framework that inherits consistency priors for reliable alignment.

Video prior for editing task. Video generative models [3, 30, 32, 33, 36, 40, 50, 58] offer strong temporal consistency priors that can be effectively transferred to image editing. Existing explorations fall into two main directions: utilizing video data for training data curation [9, 13, 60] and leveraging video models for inference-time guidance [46, 59]. While effective for enhancing single-image quality or ensuring short-range consistency, these methods do not solve the fundamental challenge of *Group-Image Editing* across diverse static views.

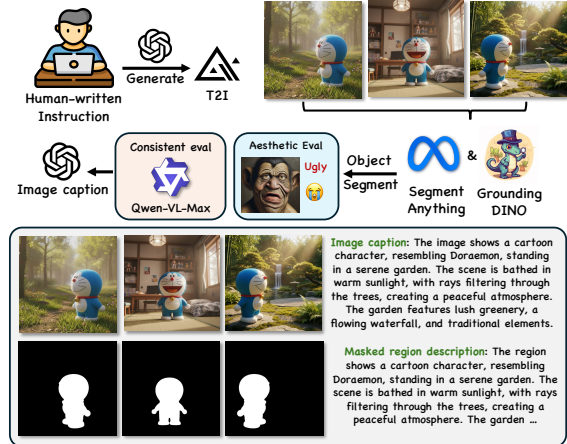


Figure 2. **Data curation pipeline.** Our pipeline processes human-written instructions through text-to-image generation, followed by quality evaluation (consistency and aesthetic assessment) and annotation generation (object segmentation and text description). The pipeline automatically produces high-quality training pairs with precise masks and detailed captions.

3. Method

We present **GroupEditing**, a training-based framework for consistent group-image editing that reformulates a set of related images as pseudo-temporal frames. To support large-scale training, we develop a data curation pipeline that automatically generates high-quality training pairs, described in Sec. 3.1. For fine-grained spatial alignment, we introduce **Ge-RoPE** to improve alignment between VGGT features and latent features by incorporating spatial disparity information with confidence levels (See Sec. 3.2.2). For identity preservation, we propose **Identity-RoPE** to maintain identity consistency across the group through precise pixel-level alignment within each image (Sec. 3.2.3). An overview of the framework is illustrated in Fig. 3.

3.1. Data curation

To facilitate large-scale training of GroupEditing, we develop a scalable data curation pipeline that automatically generates high-quality training pairs with precise masks and detailed text descriptions. The pipeline, illustrated in Fig. 2, consists of three main stages: image generation, quality evaluation, and annotation generation.

3.1.1. Group image generation

Given a set of human-written text instructions $\mathcal{C} = \{c^{(n)}\}_{n=1}^N$, we employ Gemini 2.5 [12] as the text-to-image (T2I) generation model to produce corresponding image sets $\mathcal{I} = \{I^{(n)}\}_{n=1}^N$, where each $I^{(n)} = \{I_t^{(n)}\}_{t=1}^T$ represents a group of related images generated from the same instruction $c^{(n)}$. The T2I model generates diverse images that share semantic content while exhibiting variations in

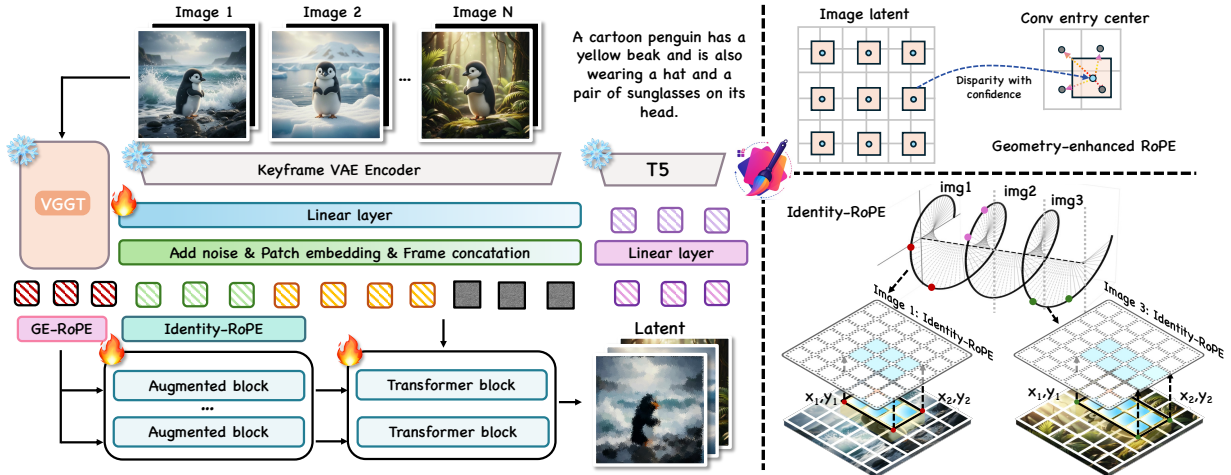


Figure 3. **Overview of proposed method.** Given a series of images and their corresponding masks, we propose a novel framework for editing while ensuring the consistency of multiple images. To achieve fine-grained spatial alignment, we introduce Geometry-enhanced RoPE (GE-RoPE), which enhances the model’s ability to maintain consistent spatial relationships across different frames, and Identity-RoPE for better consistent identity preservation.

viewpoint, pose, or scene composition, naturally forming pseudo-temporal sequences suitable for group-image editing training. In total, 18248 instruction–image groups are generated for subsequent processing.

3.1.2. Quality evaluation

Upon obtaining the generated images, we first perform object segmentation to extract precise masks before conducting quality evaluation. Object segmentation is performed using a combination of Segment Anything [25] and Grounding DINO [28]. Segment Anything provides fine-grained segmentation masks for objects and regions of interest, generating pixel-level masks $M_t^{(n)} \in [0, 1]^{H \times W}$ for each image $I_t^{(n)}$. Grounding DINO enables semantic grounding by associating text descriptions with corresponding image regions, facilitating the identification of semantically meaningful objects and their spatial locations. After object grounding and segmentation, 17618 instruction–image groups remain with valid object–mask pairs.

For each image with its corresponding segmentation mask, we perform quality evaluation using a multi-stage pipeline. First, we generate a detailed image caption $s_t^{(n)}$ for each image $I_t^{(n)}$ using a vision-language model, providing rich semantic descriptions of the image content. The image captions are then fed into a consistency evaluation module based on Qwen-VL-Max [57], which assesses the semantic consistency and coherence of the generated image set $\{I_t^{(n)}\}_{t=1}^{T^{(n)}}$ with respect to the instruction $c^{(n)}$. Images that fail to meet the consistency threshold are filtered out from the training dataset. During this process, 7982 groups passed the semantic and aesthetic evaluation stages.

Subsequently, an aesthetic evaluation module [48] as-

sesses the visual quality of each image, identifying and removing images with poor aesthetic quality or visual artifacts. This ensures that the training dataset contains only high-quality images that contribute positively to model learning. Finally, a total of 7517 high-quality data groups are filtered to form our final training set.

3.1.3. Annotation generation

For each image that passes both consistency and aesthetic evaluation, we generate comprehensive text annotations. Using the image captions $s_t^{(n)}$ already generated during the quality evaluation stage, we retain the full image captions for the passed images. Additionally, for each segmented region identified by the masks $M_t^{(n)}$, we generate masked region descriptions $d_t^{(n)}$ that describe the content within the masked area, enabling fine-grained semantic understanding at both the image level and the region level.

The final training dataset consists of image groups $\{I_t^{(n)}\}_{t=1}^{T^{(n)}}$ paired with their corresponding masks $\{M_t^{(n)}\}_{t=1}^{T^{(n)}}$, image captions $\{s_t^{(n)}\}_{t=1}^{T^{(n)}}$, and masked region descriptions $\{d_t^{(n)}\}_{t=1}^{T^{(n)}}$. This comprehensive annotation enables the model to learn both semantic alignment and geometric consistency across image groups, supporting the training of GroupEditing’s implicit-explicit correspondence fusion mechanism.

3.2. Group Editing

3.2.1. Pipeline overview

As illustrated in the left part of Fig. 3, the pipeline processes an input image sequence $\{I_t\}_{t=1}^T$ through several stages. A fixed latent map $\mathcal{Z} : \mathbb{R}^{H \times W \times 3} \rightarrow \mathbb{R}^{C \times H' \times W'}$ encodes



Figure 4. **Visual illustration about correspondence using VGGT.** Comparisons of the input and our correspondence prediction using VGGT. The results without VGGT show less accurate alignment, while the inclusion of VGGT improves consistency and precision in the correspondence.

each frame: $z_t = \mathcal{Z}(I_t)$. At the scheduler parameter $\tau \in [0, 1]$, noisy latents are constructed as:

$$x_t(\tau) = \alpha(\tau)z_t + \sigma(\tau)\epsilon, \quad \epsilon \sim \mathcal{N}(0, \mathbf{I}). \quad (1)$$

The latents are patchified with patch size (p_t, p_h, p_w) into token sequences of length $S = \frac{T H' W'}{p_t p_h p_w}$. Text condition c is encoded by a T5 encoder into contextual embeddings $u = \mathcal{E}_c(c) \in \mathbb{R}^{L \times D_c}$.

For positional encoding, we apply Identity-RoPE to obtain the baseline 2D spatial positional map $\Pi_{\text{Id}}(t, h, w)$ for the latent tokens, which provides precise pixel-level alignment within each image. When a displacement field Δ is available, we apply Ge-RoPE to obtain the geometry-aware positional map $\Pi_{\text{Ge}}(t, h, w)$ that adjusts spatial indices according to Δ .

Explicit dense tokens $G \in \mathbb{R}^{F \times H_g \times W_g \times D}$ are extracted from VGGT over the input set, with a positional map Π_G defined on the (F, H_g, W_g) grid. These tokens are augmented internally to the latent token sequence within each transformer block before self-interaction:

$$\tilde{X} = [X_{\text{latent}}, G], \quad \tilde{\Pi} = [\Pi, \Pi_G], \quad (2)$$

where X_{latent} denotes the patchified latent tokens, Π is either Π_{Id} or Π_{Ge} depending on the availability of Δ , and Π_G is the positional map for VGGT tokens obtained by mapping the backbone’s per-axis frequency banks to the (F, H_g, W_g) grid. The augmented sequence is processed through self-attention with the fused positional encoding $\tilde{\Pi}$, followed by cross-attention to u , and feed-forward layers. After self-attention, the output is truncated back to the original latent token dimensionality (only X_{latent} tokens are retained), ensuring that subsequent operations and integration remain in the latent space while benefiting from the cross-view constraints provided by G . The backbone predicts a

velocity field:

$$\hat{v}_\theta(x_t(\tau), c, u, \Pi, G, \Pi_G; \tau) \in \mathbb{R}^{C \times H' \times W'}, \quad (3)$$

which is integrated along the scheduler trajectory to obtain edited latents $\{\tilde{z}_t\}$, decoded \mathcal{Z}^{-1} to produce images $\{\tilde{I}_t\}$.

Algorithm 1 Identity-RoPE for pixel alignment

Require: Base frequency $\theta \in \mathbb{R}_{>0}$, embedding dimensions $D_t, D_h, D_w \in \mathbb{N}$, number of images $T \in \mathbb{N}$, spatial dimensions $H', W' \in \mathbb{N}$, object masks $\{M_t\}_{t=1}^T$ where $M_t \in [0, 1]^{H' \times W'}$

Ensure: Positional encoding $\Pi_{\text{Id}} \in \mathbb{C}^{(T \times H' \times W') \times D/2}$ where $D = D_t + D_h + D_w$

```

1: for  $t = 1$  to  $T$  do
2:    $x_1^{(t)} \leftarrow \min_{(h,w) \in \{M_t > 0.5\}} w$ 
3:    $y_1^{(t)} \leftarrow \min_{(h,w) \in \{M_t > 0.5\}} h$ 
4:    $x_2^{(t)} \leftarrow \max_{(h,w) \in \{M_t > 0.5\}} w$ 
5:    $y_2^{(t)} \leftarrow \max_{(h,w) \in \{M_t > 0.5\}} h$ 
6: end for

7: for  $k \in \{h, w, t\}$  do
8:    $\mathbf{d}_k \leftarrow [0, 1, \dots, D_k/2 - 1]^T \in \mathbb{N}^{D_k/2}$ 
9:    $\mathbf{f}_k \leftarrow \theta^{-2\mathbf{d}_k/D_k} \in \mathbb{R}^{D_k/2}$ 
10:   $\mathbf{p}_k \leftarrow [0, 1, \dots, S_k - 1]^T$  where  $S_k \in \{H', W', T\}$ 
11:   $\Phi_k \leftarrow \exp(\text{ip}_k \mathbf{f}_k^T) \in \mathbb{C}^{S_k \times D_k/2}$ 
12: end for

13: for  $t = 1$  to  $T$  do
14:   for  $(h, w) \in [0, H' - 1] \times [0, W' - 1]$  do
15:     if  $x_1^{(t)} \leq w \leq x_2^{(t)} \wedge y_1^{(t)} \leq h \leq y_2^{(t)}$  then
16:        $\tilde{h} \leftarrow h - y_1^{(t)}, \tilde{w} \leftarrow w - x_1^{(t)}$ 
17:     else
18:        $\tilde{h} \leftarrow h, \tilde{w} \leftarrow w$ 
19:     end if
20:      $\Phi_h^{(t)}(h, w) \leftarrow \Phi_h(\tilde{h}), \Phi_w^{(t)}(h, w) \leftarrow \Phi_w(\tilde{w})$ 
21:   end for
22: end for

23:  $\Phi_t \leftarrow \Phi_t \otimes \mathbf{1}_{H'} \otimes \mathbf{1}_{W'} \in \mathbb{C}^{T \times H' \times W' \times D_t/2}$ 
24:  $\Phi_h \leftarrow \mathbf{1}_T \otimes \Phi_h \otimes \mathbf{1}_{W'} \in \mathbb{C}^{T \times H' \times W' \times D_h/2}$ 
25:  $\Phi_w \leftarrow \mathbf{1}_T \otimes \mathbf{1}_{H'} \otimes \Phi_w \in \mathbb{C}^{T \times H' \times W' \times D_w/2}$ 
26:  $\Phi \leftarrow \text{concat}(\Phi_t, \Phi_h, \Phi_w) \in \mathbb{C}^{T \times H' \times W' \times D/2}$ 
27:  $\Pi_{\text{Id}} \leftarrow \text{reshape}(\Phi, (T \times H' \times W', D/2))$ 
28: return  $\Pi_{\text{Id}}$ 

```

3.2.2. Geometry-enhanced RoPE (Ge-RoPE)

The top-right part of Fig. 3 and Fig. 4 illustrate Ge-RoPE, which improves alignment between VGGT features and latent features by incorporating spatial disparity information with confidence levels from displacement fields. Given a

displacement field $\Delta(h, w) = (\Delta_h, \Delta_w) \in \mathbb{R}^{2 \times H' \times W'}$ that encodes pixel-level correspondences, confidence is derived from disparity magnitude (larger values indicate higher confidence), following a depth-disparity relationship similar to depth-based forward splatting [64]. The displacement field is resized to match latent resolution (H', W') using bilinear interpolation, divided by the patch size (typically 16), and smoothed independently for h and w components using a 2D Gaussian kernel ($\mu = 21, \sigma = 11$) to prioritize high-confidence correspondences.

We construct warped spatial grids by adding the smoothed displacement to original grid indices: $\tilde{h}(h, w) = h + \Delta_h^{\text{smooth}}(h, w)$ and $\tilde{w}(h, w) = w + \Delta_w^{\text{smooth}}(h, w)$, clamped to $[0, H' - 1]$ and $[0, W' - 1]$ respectively. These warped grids index the precomputed frequency banks using nearest neighbor indexing, resulting in geometry-aware frequency tensors Φ_h^{Ge} and Φ_w^{Ge} . The temporal component remains unchanged: $\Phi_t^{\text{Ge}} = \Phi_t$. The final Ge-RoPE encoding is:

$$\Pi_{\text{Ge}} = \text{concat}(\Phi_t, \Phi_h^{\text{Ge}}, \Phi_w^{\text{Ge}}) \in \mathbb{C}^{S_t \times S_h \times S_w \times D/2}. \quad (4)$$

Applied to queries and keys through multiplication:

$$q' = \text{Re}(q^{\text{C}} \odot \Pi_{\text{Ge}}), \quad k' = \text{Re}(k^{\text{C}} \odot \Pi_{\text{Ge}}), \quad (5)$$

where \odot denotes element-wise complex multiplication, $q^{\text{C}}, k^{\text{C}}$ are complex representations of queries and keys (reshaped from real vectors), and $\text{Re}(\cdot)$ extracts the real part. This warping aligns latent token positional encodings with the geometric structure in VGGT features.

3.2.3. Identity-RoPE

The bottom-right part of Fig. 3 illustrates Identity-RoPE, which maintains identity consistency across the group through precise pixel-level alignment within each image via a 2D spatial positional encoding. Identity-RoPE applies separate 1D RoPE components for height and width using precomputed frequency banks. The frequencies are $\omega_h^{(i)} = \theta^{-2i/D_h}$ and $\omega_w^{(i)} = \theta^{-2i/D_w}$ for $i \in \{0, 1, \dots, D_h/2 - 1\}$ and $i \in \{0, 1, \dots, D_w/2 - 1\}$ respectively, where θ is the base frequency. For spatial position (h, w) where $h \in \{0, 1, \dots, H' - 1\}$ and $w \in \{0, 1, \dots, W' - 1\}$, the 1D RoPE components are:

$$\begin{aligned} \Phi_h(h) &= \exp(i\omega_h \cdot h) \in \mathbb{C}^{D_h/2}, \\ \Phi_w(w) &= \exp(i\omega_w \cdot w) \in \mathbb{C}^{D_w/2}, \end{aligned} \quad (6)$$

where $\omega_h = [\omega_h^{(0)}, \omega_h^{(1)}, \dots, \omega_h^{(D_h/2-1)}]^T$ and $\omega_w = [\omega_w^{(0)}, \omega_w^{(1)}, \dots, \omega_w^{(D_w/2-1)}]^T$ are frequency vectors, and i is the imaginary unit.

For robust identity alignment, we use a bounding rectangle-based matching strategy. For each image t , we compute the smallest bounding rectangle $\mathcal{R}_t =$

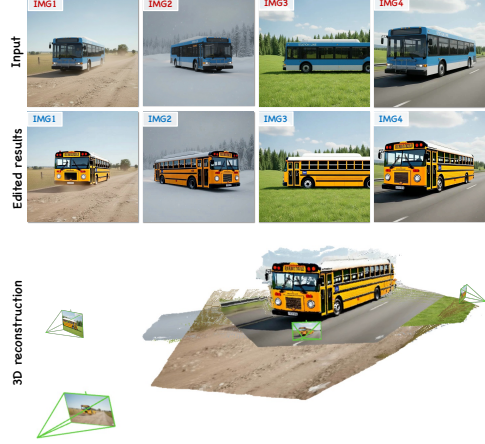


Figure 5. **3D reconstruction using editing results.** The top row shows input images, the middle row displays the edited results, and the bottom row demonstrates 3D reconstruction using Must3R, aligning 2D points to create a 3D model of the modified bus.

$\{(x_1^{(t)}, y_1^{(t)}), (x_2^{(t)}, y_2^{(t)})\}$ from the segmentation mask M_t , where $(x_1^{(t)}, y_1^{(t)})$ and $(x_2^{(t)}, y_2^{(t)})$ are the bottom-left and top-right corners. Spatial coordinates are determined conditionally:

$$(\tilde{h}, \tilde{w}) = \begin{cases} (h - y_1^{(t)}, w - x_1^{(t)}) & \text{if } (h, w) \in \mathcal{R}_t \\ (h, w) & \text{otherwise} \end{cases} \quad (7)$$

where $\mathcal{R}_t = \{(h, w) : x_1^{(t)} \leq w \leq x_2^{(t)} \wedge y_1^{(t)} \leq h \leq y_2^{(t)}\}$. Pixels within \mathcal{R}_t use normalized coordinates relative to the rectangle’s origin, ensuring corresponding object regions share identical positional encodings regardless of absolute positions. The complete positional encoding is:

$$\Pi_{\text{Id}}(t, h, w) = \text{concat}(\Phi_t(t), \Phi_h(\tilde{h}), \Phi_w(\tilde{w})) \in \mathbb{C}^{D/2}, \quad (8)$$

where $\Phi_t(t)$ is the temporal encoding component, and $D = D_t + D_h + D_w$. Applied to queries and keys:

$$q' = \text{Re}(q^{\text{C}} \odot \Pi_{\text{Id}}), \quad k' = \text{Re}(k^{\text{C}} \odot \Pi_{\text{Id}}), \quad (9)$$

where \odot denotes element-wise complex multiplication. This ensures tokens within corresponding object regions share consistent positional signatures, as visualized in the bottom-right part of Fig. 3.

4. Experiment

4.1. Implementation Details

We train our model using on WAN-2.1 [53], a transformer-based video diffusion model [16, 26, 49]. The optimization is performed using AdamW [31] with a weight decay of 0.01 and an initial learning rate of 1×10^{-4} . Training is conducted at a spatial resolution of 528×528 and a batch size

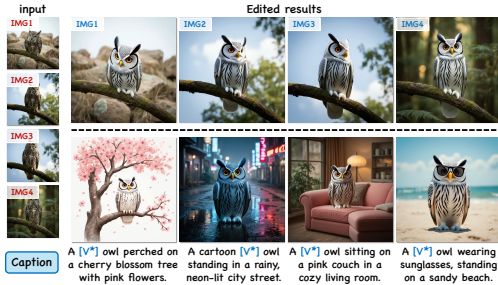


Figure 6. **Image customization using editing results.** Customized generation is achieved by embedding the edited concepts into the generative model, leveraging the outputs from our consistent editing method.

of 8 on 8 NVIDIA A800 GPUs under PyTorch. More implementation details and quantitative metrics are provided in the supplementary materials.

4.2. Applications

Image customization based on the consistent results. To demonstrate the practical application of our consistent editing method, we use DreamBooth [47] and Low-Rank Adaptation (LoRA) [19] for customized image generation. By leveraging the edited outputs from our method, we finetune a generative model with DreamBooth for 600 steps. As shown in Fig. 6, the fine-tuned model successfully generates images based on the edited images, enabling both novel concept generation and editing.

3D reconstruction based on the consistent results. Our method also benefits 3D reconstruction by leveraging the Must3R [5] to predict accurate 3D scene representations from consistent image pairs. Using the edited images as inputs, Must3R generates 3D point-based models and 2D matchings without requiring additional inputs like camera parameters. As shown in Fig. 5, the reconstruction results confirm the editing consistency for the four sets of edits.

4.3. Comparison with baselines.

Qualitative comparison. We present a qualitative evaluation of our approach with recent open-sourced state-of-the-art methods in local image editing. We compare our method with open-sourced approaches such as Anydoor [8], Paint-by-Example [61], OminiControl [51], and Edicho [3]. The visual results are shown in Fig. 7. Anydoor [8], OminiControl [51], and Edicho [3] struggle to edit multiple images coherently. Our framework enables editing the image group consistently. Additionally, we show the visual comparison with Masactrl [6], StyleAligned [17], Edicho [3], and OminiControl [51] in global image editing. As shown in Fig. 7, our approach demonstrates superior consistency and alignment across the multiple editing results.

Quantitative comparison. We compare our method with

state-of-the-art image editing on the collected benchmark, GroupEditBench. It includes 800 image sets generated by a powerful T2I diffusion model. The GroupEditBench includes diverse content, including objects, humans, animals, and landscapes, and various styles of images, such as sketch and cyberpunk style. We split them into local and global image editing. For local image editing, we compare our framework with Anydoor [8], OminiControl [51], Edicho [3]. for global image editing, StyleAligned [17], OminiControl [51] and Edicho [3] are considered to fair comparison. We evaluate these methods using several standard metrics (shown in Tab. 1 and Tab. 2). For “Editing Consis.,” following Edicho, we use the feature similarity of the edited results to evaluate the editing consistency. We leverage the Laion-Aesthetic Score Predictor [48] for Aesthetic-Score. Additionally, we invited 20 volunteers to rank methods across four aspects, including identity consistency, aesthetic, appearance fidelity, and overall quality, on a 1 (best) to 4 scale. The average rank (lower is better) is shown in Tab. 1. Our method achieves the top result in both automatic metrics and human preference.

4.4. Ablation study

Effectiveness of Geometry-enhanced RoPE. We ablate various geometry-enhanced RoPE (Relative Positional Encoding) configurations during training. The visual results are provided in Fig. 8. As the geometry-enhanced RoPE is applied, we observe the improvements in the model’s spatial awareness and the accuracy of geometric transformations. Additionally, as shown in Tab. 3, we report the quantitative ablation results to further validate the effectiveness of geometry-enhanced RoPE.

Effectiveness of Identity-RoPE. Thanks to our Identity-RoPE, the model can maintain a more consistent and stable representation of the object’s identity. In Fig. 8, we observe that the object’s identity remains significantly more consistent when equipping the Identity-RoPE layers. As shown in Tab. 3, our experiments quantitatively validate the benefit of incorporating Identity-RoPE in preserving identity consistency across different images.

5. Conclusion

In this paper, we present GroupEditing, a novel framework designed to address the challenges of consistent multiple-image editing. By leveraging explicit geometric correspondences from VGGT with implicit priors from pre-trained video models, our method not only ensures accurate modifications but also maintains identity preservation across diverse images through the alignment-enhanced RoPE module. To support large-scale training, the framework is backed by GroupEditData, a new dataset that provides high-quality image groups with precise segmentation masks and detailed image captions. Additionally, we evaluate Group

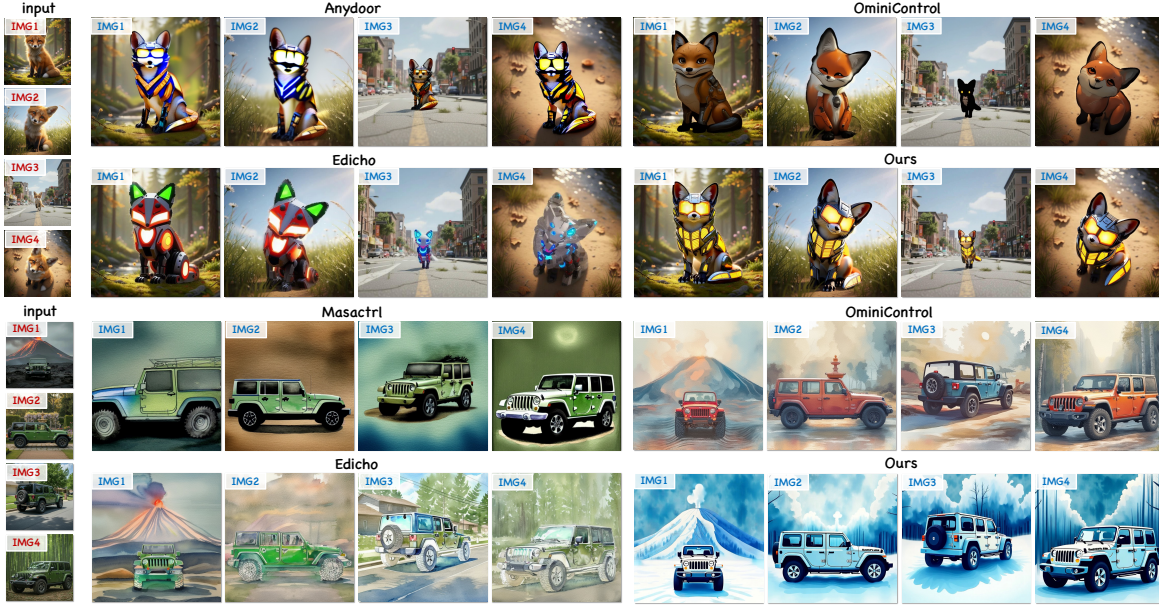


Figure 7. **Visual comparison with SOTA image editing on local and global editing**. The top row shows results for different methods on local edits. The bottom row presents our method alongside other techniques for global editing. Our approach demonstrates superior consistency and high-quality edits across both local and global changes. The text prompts are “A cartoon fox with futuristic robotic armor and orange details.” and “A jeep vehicle in outdoor settings, including snow-covered style, rendered in soft watercolor painting style.”.

Table 1. **Comparison with state-of-the-art image editing on local editing**. Red and Blue denote the best and second best results.

Method	Quantitative metrics					User study			
	CLIP-Score \uparrow	Aesthetic-Score \uparrow	DINO-Score \uparrow	Editing Consis. \uparrow	PSNR \uparrow	Iden. Consis. \downarrow	Aesthetic. \downarrow	App. Fidelity \downarrow	Overall \downarrow
Anydoor [8]	0.2728	4.72	0.7208	0.8697	0.6182	3.56	3.23	3.60	3.32
OminiControl [51]	0.2902	5.10	0.7326	0.8676	0.6457	2.84	2.84	1.96	2.66
Edicho [3]	0.3059	4.89	0.8080	0.8988	0.6935	1.93	2.47	2.93	1.95
Ours	0.3122	5.39	0.8168	0.9239	0.7624	1.67	1.46	1.50	1.47

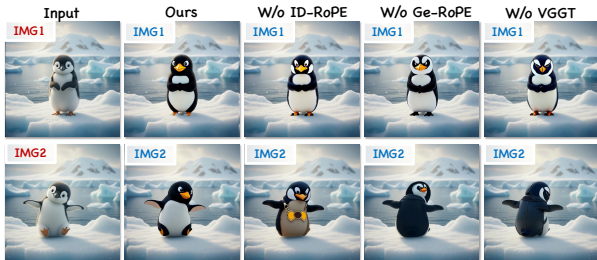


Figure 8. **Visual ablation about proposed modules**. We provide a visual ablation study on the effectiveness of various mechanisms. The prompt is “The penguin has a black and white body with orange feet and beak.”

pEditing using GroupEditBench, a comprehensive benchmark specifically designed to assess group-level editing performance. Extensive experimental results demonstrate that GroupEditing outperforms SOTA methods, including visual quality, editing consistency, and semantic alignment, estab-

Table 2. **Comparison with state-of-the-art image editing on global editing**. Red and Blue denote the best and second best results, respectively.

Method	Quantitative metrics			
	CLIP-Score \uparrow	Aesthetic-Score \uparrow	DINO-Score \uparrow	Editing Consis. \uparrow
StyleAligned [17]	0.2910	4.75	0.8645	0.8714
Edicho [3]	0.2920	4.59	0.8714	0.8859
OminiControl [51]	0.2918	4.94	0.8553	0.8965
Ours	0.2987	5.48	0.9287	0.9147

Table 3. **Quantitative ablation**. Red and Blue denote the best and second best results, respectively.

Method	Quantitative metrics			
	CLIP-Score \uparrow	Aesthetic-Score \uparrow	DINO-Score \uparrow	Editing Consis. \uparrow
W/o VGGT [17]	0.2728	4.72	0.7208	0.8616
W/o Ge-RoPE [3]	0.2902	4.89	0.7326	0.8697
W/o Identity-RoPE [51]	0.2902	4.89	0.7326	0.9108
Ours	0.3122	5.39	0.8168	0.9239

lishing it as a promising solution for a wide range of multi-image editing applications.

References

- [1] Omri Avrahami, Dani Lischinski, and Ohad Fried. Blended diffusion for text-driven editing of natural images. In *Proceedings of the IEEE/CVF conference on computer vision and pattern recognition*, pages 18208–18218, 2022. 3
- [2] Omri Avrahami, Amir Hertz, Yael Vinker, Moab Arar, Shlomi Fruchter, Ohad Fried, Daniel Cohen-Or, and Dani Lischinski. The chosen one: Consistent characters in text-to-image diffusion models. In *ACM SIGGRAPH 2024 conference papers*, pages 1–12, 2024. 2
- [3] Qingyan Bai, Hao Ouyang, Yinghao Xu, Qiuyu Wang, Ceyuan Yang, Ka Leong Cheng, Yujun Shen, and Qifeng Chen. Edicho: Consistent image editing in the wild. In *Proceedings of the IEEE/CVF International Conference on Computer Vision*, pages 15277–15287, 2025. 2, 3, 7, 8
- [4] Tim Brooks, Aleksander Holynski, and Alexei A Efros. Instructpix2pix: Learning to follow image editing instructions. In *Proceedings of the IEEE/CVF conference on computer vision and pattern recognition*, pages 18392–18402, 2023. 2, 3
- [5] Johann Cabon, Lucas Stoffl, Leonid Antsfeld, Gabriela Csurka, Boris Chidlovskii, Jerome Revaud, and Vincent Leroy. Must3r: Multi-view network for stereo 3d reconstruction. In *Proceedings of the Computer Vision and Pattern Recognition Conference*, pages 1050–1060, 2025. 7
- [6] Mingdeng Cao, Xintao Wang, Zhongang Qi, Ying Shan, Xiaohu Qie, and Yinqiang Zheng. Masactrl: Tuning-free mutual self-attention control for consistent image synthesis and editing. In *Proceedings of the IEEE/CVF international conference on computer vision*, pages 22560–22570, 2023. 3, 7
- [7] Xi Chen, Yutong Feng, Mengting Chen, Yiyang Wang, Shilong Zhang, Yu Liu, Yujun Shen, and Hengshuang Zhao. Zero-shot image editing with reference imitation. *Advances in Neural Information Processing Systems*, 37:84010–84032, 2024. 2, 3
- [8] Xi Chen, Lianghua Huang, Yu Liu, Yujun Shen, Deli Zhao, and Hengshuang Zhao. Anydoor: Zero-shot object-level image customization. In *Proceedings of the IEEE/CVF conference on computer vision and pattern recognition*, pages 6593–6602, 2024. 7, 8
- [9] Xi Chen, Zhifei Zhang, He Zhang, Yuqian Zhou, Soo Ye Kim, Qing Liu, Yijun Li, Jianming Zhang, Nanxuan Zhao, Yilin Wang, et al. Unireal: Universal image generation and editing via learning real-world dynamics. In *Proceedings of the Computer Vision and Pattern Recognition Conference*, pages 12501–12511, 2025. 3
- [10] Yiyang Chen, Xuanhua He, Xiujuan Ma, and Yue Ma. Contextflow: Training-free video object editing via adaptive context enrichment. *arXiv preprint arXiv:2509.17818*, 2025. 2
- [11] Yu-Sheng Chen, Yu-Ching Wang, Man-Hsin Kao, and Yung-Yu Chuang. Deep photo enhancer: Unpaired learning for image enhancement from photographs with gans. In *Proceedings of the IEEE conference on computer vision and pattern recognition*, pages 6306–6314, 2018. 2
- [12] Gheorghe Comanici, Eric Bieber, Mike Schaekermann, Ice Pasupat, Noveen Sachdeva, Inderjit Dhillon, Marcel Blisstein, Ori Ram, Dan Zhang, Evan Rosen, et al. Gemini 2.5: Pushing the frontier with advanced reasoning, multimodality, long context, and next generation agentic capabilities. *arXiv preprint arXiv:2507.06261*, 2025. 2, 3
- [13] Chaorui Deng, Deyao Zhu, Kunchang Li, Chenhui Gou, Feng Li, Zeyu Wang, Shu Zhong, Weihao Yu, Xiaonan Nie, Ziang Song, et al. Emerging properties in unified multimodal pretraining. *arXiv preprint arXiv:2505.14683*, 2025. 3
- [14] Kunyu Feng, Yue Ma, Bingyuan Wang, Chenyang Qi, Haozhe Chen, Qifeng Chen, and Zeyu Wang. Dit4edit: Diffusion transformer for image editing. In *Proceedings of the AAAI Conference on Artificial Intelligence*, pages 2969–2977, 2025. 3
- [15] Ian J Goodfellow, Jean Pouget-Abadie, Mehdi Mirza, Bing Xu, David Warde-Farley, Sherjil Ozair, Aaron Courville, and Yoshua Bengio. Generative adversarial nets. *Advances in neural information processing systems*, 27, 2014. 3
- [16] Yoav HaCohen, Nisan Chiprut, Benny Brazowski, Daniel Shalem, Dudu Moshe, Eitan Richardson, Eran Levin, Guy Shiran, Nir Zabari, Ori Gordon, Poriya Panet, Sapir Weissbuch, Victor Kulikov, Yaki Bitterman, Zeev Melumian, and Ofir Bibi. Ltx-video: Realtime video latent diffusion. *arXiv preprint arXiv:2501.00103*, 2024. 6
- [17] Amir Hertz, Andrey Voynov, Shlomi Fruchter, and Daniel Cohen-Or. Style aligned image generation via shared attention. In *Proceedings of the IEEE/CVF Conference on Computer Vision and Pattern Recognition*, pages 4775–4785, 2024. 7, 8
- [18] Jonathan Ho, Ajay Jain, and Pieter Abbeel. Denoising diffusion probabilistic models. *Advances in neural information processing systems*, 33:6840–6851, 2020. 3
- [19] Edward J Hu, Yelong Shen, Phillip Wallis, Zeyuan Allen-Zhu, Yuanzhi Li, Shean Wang, Lu Wang, Weizhu Chen, et al. Lora: Low-rank adaptation of large language models. *ICLR*, 1(2):3, 2022. 7
- [20] Yi Huang, Jiancheng Huang, Yifan Liu, Mingfu Yan, Jiayi Lv, Jianzhuang Liu, Wei Xiong, He Zhang, Liangliang Cao, and Shifeng Chen. Diffusion model-based image editing: A survey. *IEEE Transactions on Pattern Analysis and Machine Intelligence*, 2025. 3
- [21] Xuan Ju, Xian Liu, Xintao Wang, Yuxuan Bian, Ying Shan, and Qiang Xu. Brushnet: A plug-and-play image inpainting model with decomposed dual-branch diffusion. In *European Conference on Computer Vision*, pages 150–168. Springer, 2024. 2
- [22] Bernhard Kerbl, Georgios Kopanas, Thomas Leimkühler, and George Drettakis. 3d gaussian splatting for real-time radiance field rendering. *ACM Trans. Graph.*, 42(4):139–1, 2023. 2
- [23] Gwanghyun Kim, Taesung Kwon, and Jong Chul Ye. Diffusionclip: Text-guided diffusion models for robust image manipulation. In *Proceedings of the IEEE/CVF conference on computer vision and pattern recognition*, pages 2426–2435, 2022. 3
- [24] Diederik P Kingma and Max Welling. Auto-encoding variational bayes. *arXiv preprint arXiv:1312.6114*, 2013. 3

- [25] Alexander Kirillov, Eric Mintun, Nikhila Ravi, Hanzi Mao, Chloe Rolland, Laura Gustafson, Tete Xiao, Spencer Whitehead, Alexander C Berg, Wan-Yen Lo, et al. Segment anything. In *Proceedings of the IEEE/CVF international conference on computer vision*, pages 4015–4026, 2023. 2, 4
- [26] Weijie Kong, Qi Tian, Zijian Zhang, Rox Min, Zuozhuo Dai, Jin Zhou, Jiangfeng Xiong, Xin Li, Bo Wu, Jianwei Zhang, et al. Hunyuanvideo: A systematic framework for large video generative models. *arXiv preprint arXiv:2412.03603*, 2024. 6
- [27] Guanzhou Lan, Qianli Ma, Yuqi Yang, Zhigang Wang, Dong Wang, Xuelong Li, and Bin Zhao. Efficient diffusion as low light enhancer. In *Proceedings of the Computer Vision and Pattern Recognition Conference*, pages 21277–21286, 2025. 3
- [28] Shilong Liu, Zhaoyang Zeng, Tianhe Ren, Feng Li, Hao Zhang, Jie Yang, Qing Jiang, Chunyuan Li, Jianwei Yang, Hang Su, et al. Grounding dino: Marrying dino with grounded pre-training for open-set object detection. In *European conference on computer vision*, pages 38–55. Springer, 2024. 2, 4
- [29] Yang Liu, Cheng Yu, Lei Shang, Ziheng Wu, Xingjun Wang, Yuze Zhao, Lin Zhu, Chen Cheng, Weitao Chen, Chao Xu, Haoyu Xie, Yuan Yao, Wenmeng Zhou, Chen Yingda, Xuansong Xie, and Baigui Sun. Facechain: A playground for identity-preserving portrait generation. *arXiv preprint arXiv:2308.14256*, 2023. 2
- [30] Zeqian Long, Mingzhe Zheng, Kunyu Feng, Xinhua Zhang, Hongyu Liu, Harry Yang, Linfeng Zhang, Qifeng Chen, and Yue Ma. Follow-your-shape: Shape-aware image editing via trajectory-guided region control. *arXiv preprint arXiv:2508.08134*, 2025. 3
- [31] Ilya Loshchilov and Frank Hutter. Decoupled weight decay regularization. *arXiv preprint arXiv:1711.05101*, 2017. 6
- [32] Qianli Ma, Xuefei Ning, Dongrui Liu, Li Niu, and Linfeng Zhang. Decouple-then-merge: Finetune diffusion models as multi-task learning. In *Proceedings of the Computer Vision and Pattern Recognition Conference*, pages 23281–23291, 2025. 3
- [33] Yue Ma, Yali Wang, Yue Wu, Ziyu Lyu, Siran Chen, Xiu Li, and Yu Qiao. Visual knowledge graph for human action reasoning in videos. In *Proceedings of the 30th ACM International Conference on Multimedia*, pages 4132–4141, 2022. 3
- [34] Yue Ma, Yingqing He, Xiaodong Cun, Xintao Wang, Siran Chen, Xiu Li, and Qifeng Chen. Follow your pose: Pose-guided text-to-video generation using pose-free videos. In *Proceedings of the AAAI Conference on Artificial Intelligence*, pages 4117–4125, 2024. 3
- [35] Yue Ma, Hongyu Liu, Hongfa Wang, Heng Pan, Yingqing He, Junkun Yuan, Ailing Zeng, Chengfei Cai, Heung-Yeung Shum, Wei Liu, et al. Follow-your-emoji: Fine-controllable and expressive freestyle portrait animation. In *SIGGRAPH Asia 2024 Conference Papers*, pages 1–12, 2024. 2
- [36] Yue Ma, Kunyu Feng, Zhongyuan Hu, Xinyu Wang, Yucheng Wang, Mingzhe Zheng, Xuanhua He, Chenyang Zhu, Hongyu Liu, Yingqing He, et al. Controllable video generation: A survey. *arXiv preprint arXiv:2507.16869*, 2025. 3
- [37] Yue Ma, Kunyu Feng, Xinhua Zhang, Hongyu Liu, David Junhao Zhang, Jinbo Xing, Yinhan Zhang, Ayden Yang, Zeyu Wang, and Qifeng Chen. Follow-your-creation: Empowering 4d creation through video inpainting. *arXiv preprint arXiv:2506.04590*, 2025. 3
- [38] Yue Ma, Yingqing He, Hongfa Wang, Andong Wang, Leqi Shen, Chenyang Qi, Jixuan Ying, Chengfei Cai, Zhifeng Li, Heung-Yeung Shum, et al. Follow-your-click: Open-domain regional image animation via motion prompts. In *Proceedings of the AAAI Conference on Artificial Intelligence*, pages 6018–6026, 2025. 2
- [39] Yue Ma, Yulong Liu, Qiyuan Zhu, Ayden Yang, Kunyu Feng, Xinhua Zhang, Zhifeng Li, Sirui Han, Chenyang Qi, and Qifeng Chen. Follow-your-motion: Video motion transfer via efficient spatial-temporal decoupled finetuning. *arXiv preprint arXiv:2506.05207*, 2025. 3
- [40] Yue Ma, Zexuan Yan, Hongyu Liu, Hongfa Wang, Heng Pan, Yingqing He, Junkun Yuan, Ailing Zeng, Chengfei Cai, Heung-Yeung Shum, et al. Follow-your-emoji-faster: Towards efficient, fine-controllable, and expressive freestyle portrait animation. *arXiv preprint arXiv:2509.16630*, 2025. 3
- [41] Yue Ma, Zhikai Wang, Tianhao Ren, Mingzhe Zheng, Hongyu Liu, Jiayi Guo, Mark Fong, Yuxuan Xue, Zixiang Zhao, Konrad Schindler, et al. Fastvmt: Eliminating redundancy in video motion transfer. *arXiv preprint arXiv:2602.05551*, 2026. 3
- [42] Ron Mokady, Amir Hertz, Kfir Aberman, Yael Pritch, and Daniel Cohen-Or. Null-text inversion for editing real images using guided diffusion models. In *Proceedings of the IEEE/CVF conference on computer vision and pattern recognition*, pages 6038–6047, 2023. 2, 3
- [43] Chong Mou, Xintao Wang, Liangbin Xie, Yanze Wu, Jian Zhang, Zhongang Qi, and Ying Shan. T2i-adapter: Learning adapters to dig out more controllable ability for text-to-image diffusion models. In *Proceedings of the AAAI conference on artificial intelligence*, pages 4296–4304, 2024. 2, 3
- [44] Or Patashnik, Rinon Gal, Daniel Cohen-Or, Jun-Yan Zhu, and Fernando De la Torre. Consolidating attention features for multi-view image editing. In *SIGGRAPH Asia 2024 Conference Papers*, pages 1–12, 2024. 3
- [45] Robin Rombach, Andreas Blattmann, Dominik Lorenz, Patrick Esser, and Björn Ommer. High-resolution image synthesis with latent diffusion models. In *Proceedings of the IEEE/CVF conference on computer vision and pattern recognition*, pages 10684–10695, 2022. 3
- [46] Noam Rotstein, Gal Yona, Daniel Silver, Roy Velich, David Bensaid, and Ron Kimmel. Pathways on the image manifold: Image editing via video generation. In *Proceedings of the Computer Vision and Pattern Recognition Conference*, pages 7857–7866, 2025. 3
- [47] Nataniel Ruiz, Yuanzhen Li, Varun Jampani, Yael Pritch, Michael Rubinstein, and Kfir Aberman. Dreambooth: Fine tuning text-to-image diffusion models for subject-driven generation. In *Proceedings of the IEEE/CVF conference*

- on computer vision and pattern recognition, pages 22500–22510, 2023. 2, 7
- [48] Christoph Schuhmann, Romain Beaumont, Richard Vencu, Cade Gordon, Ross Wightman, Mehdi Cherti, Theo Coombes, Aarush Katta, Clayton Mullis, Mitchell Wortsman, et al. Laion-5b: An open large-scale dataset for training next generation image-text models. *Advances in neural information processing systems*, 35:25278–25294, 2022. 4, 7
- [49] Team Seawead, Ceyuan Yang, Zhijie Lin, Yang Zhao, Shanchuan Lin, Zhibei Ma, Haoyuan Guo, Hao Chen, Lu Qi, Sen Wang, et al. Seaweed-7b: Cost-effective training of video generation foundation model. *arXiv preprint arXiv:2504.08685*, 2025. 6
- [50] Yutao Shen, Junkun Yuan, Toru Aonishi, Hideki Nakayama, and Yue Ma. Follow-your-preference: Towards preference-aligned image inpainting. *arXiv preprint arXiv:2509.23082*, 2025. 3
- [51] Zhenxiong Tan, Songhua Liu, Xingyi Yang, Qiaochu Xue, and Xinchao Wang. Ominicontrol: Minimal and universal control for diffusion transformer. In *Proceedings of the IEEE/CVF International Conference on Computer Vision*, pages 14940–14950, 2025. 7, 8
- [52] Narek Tumanyan, Michal Geyer, Shai Bagon, and Tali Dekel. Plug-and-play diffusion features for text-driven image-to-image translation. In *Proceedings of the IEEE/CVF conference on computer vision and pattern recognition*, pages 1921–1930, 2023. 2, 3
- [53] Team Wan, Ang Wang, Baole Ai, Bin Wen, Chaojie Mao, Chen-Wei Xie, Di Chen, Feiwei Yu, Haiming Zhao, Jianxiao Yang, Jianyuan Zeng, Jiayu Wang, Jingfeng Zhang, Jingen Zhou, Jinkai Wang, Jixuan Chen, Kai Zhu, Kang Zhao, Keyu Yan, Lianghua Huang, Mengyang Feng, Ningyi Zhang, Pandeng Li, Pingyu Wu, Ruihang Chu, Ruili Feng, Shiwei Zhang, Siyang Sun, Tao Fang, Tianxing Wang, Tianyi Gui, Tingyu Weng, Tong Shen, Wei Lin, Wei Wang, Wei Wang, Wenmeng Zhou, Wenteng Wang, Wenting Shen, Wenyuan Yu, Xianzhong Shi, Xiaoming Huang, Xin Xu, Yan Kou, Yangyu Lv, Yifei Li, Yijing Liu, Yiming Wang, Yingya Zhang, Yitong Huang, Yong Li, You Wu, Yu Liu, Yulin Pan, Yun Zheng, Yuntao Hong, Yupeng Shi, Yutong Feng, Zeyinzi Jiang, Zhen Han, Zhi-Fan Wu, and Ziyu Liu. Wan: Open and advanced large-scale video generative models. *arXiv preprint arXiv:2503.20314*, 2025. 2, 6
- [54] Jiangshan Wang, Yue Ma, Jiayi Guo, Yicheng Xiao, Gao Huang, and Xiu Li. Cove: Unleashing the diffusion feature correspondence for consistent video editing. *Advances in Neural Information Processing Systems*, 37:96541–96565, 2024. 2
- [55] Jiangshan Wang, Junfu Pu, Zhongang Qi, Jiayi Guo, Yue Ma, Nisha Huang, Yuxin Chen, Xiu Li, and Ying Shan. Taming rectified flow for inversion and editing. *arXiv preprint arXiv:2411.04746*, 2024. 3
- [56] Jianyuan Wang, Minghao Chen, Nikita Karaev, Andrea Vedaldi, Christian Rupprecht, and David Novotny. Vggt: Visual geometry grounded transformer. In *Proceedings of the Computer Vision and Pattern Recognition Conference*, pages 5294–5306, 2025. 2
- [57] Peng Wang, Shuai Bai, Sinan Tan, Shijie Wang, Zhihao Fan, Jinze Bai, Keqin Chen, Xuejing Liu, Jialin Wang, Wenbin Ge, et al. Qwen2-vl: Enhancing vision-language model’s perception of the world at any resolution. *arXiv preprint arXiv:2409.12191*, 2024. 2, 4
- [58] Daniel Winter, Matan Cohen, Shlomi Fruchter, Yael Pritch, Alex Rav-Acha, and Yedid Hoshen. Objectdrop: Bootstrapping counterfactuals for photorealistic object removal and insertion. In *European Conference on Computer Vision*, pages 112–129. Springer, 2024. 3
- [59] Jay Zhangjie Wu, Xuanchi Ren, Tianchang Shen, Tianshi Cao, Kai He, Yifan Lu, Ruiyuan Gao, Enze Xie, Shiyi Lan, Jose M Alvarez, et al. Chronoedit: Towards temporal reasoning for image editing and world simulation. *arXiv preprint arXiv:2510.04290*, 2025. 3
- [60] Shitao Xiao, Yueze Wang, Junjie Zhou, Huaying Yuan, Xingrun Xing, Ruiran Yan, Chaofan Li, Shuting Wang, Tiejun Huang, and Zheng Liu. Omnigen: Unified image generation. In *Proceedings of the Computer Vision and Pattern Recognition Conference*, pages 13294–13304, 2025. 3
- [61] Binxin Yang, Shuyang Gu, Bo Zhang, Ting Zhang, Xuejin Chen, Xiaoyan Sun, Dong Chen, and Fang Wen. Paint by example: Exemplar-based image editing with diffusion models. In *Proceedings of the IEEE/CVF conference on computer vision and pattern recognition*, pages 18381–18391, 2023. 2, 7
- [62] Xin Yu, Tianyu Wang, Soo Ye Kim, Paul Guerrero, Xi Chen, Qing Liu, Zhe Lin, and Xiaojuan Qi. Objectmover: Generative object movement with video prior. In *Proceedings of the IEEE/CVF Conference on Computer Vision and Pattern Recognition (CVPR)*, pages 17682–17691, 2025. 3
- [63] Lvmin Zhang, Anyi Rao, and Maneesh Agrawala. Adding conditional control to text-to-image diffusion models. In *Proceedings of the IEEE/CVF international conference on computer vision*, pages 3836–3847, 2023. 2, 3
- [64] Sijie Zhao, Wenbo Hu, Xiaodong Cun, Yong Zhang, Xiaoyu Li, Zhe Kong, Xiangjun Gao, Muyao Niu, and Ying Shan. Stereocrafter: Diffusion-based generation of long and high-fidelity stereoscopic 3d from monocular videos. *arXiv preprint arXiv:2409.07447*, 2024. 6
- [65] Chenyang Zhu, Kai Li, Yue Ma, Longxiang Tang, Chengyu Fang, Chubin Chen, Qifeng Chen, and Xiu Li. Instantswap: Fast customized concept swapping across sharp shape differences. *arXiv preprint arXiv:2412.01197*, 2024. 2
- [66] Chenyang Zhu, Kai Li, Yue Ma, Chunming He, and Xiu Li. Multibooth: Towards generating all your concepts in an image from text. In *Proceedings of the AAAI Conference on Artificial Intelligence*, pages 10923–10931, 2025. 2